Cell Tissue Res (2012) 350:361–372
DOI 10.1007/s00441-012-1475-8

REGULAR ARTICLE

Effects of doxorubicin cancer therapy on autophagy and the ubiquitin-proteasome system in long-term cultured adult rat cardiomyocytes

Polychronis Dimitrakis · Maria-Iris Romay-Ogando · Francesco Timolati · Thomas M. Suter · Christian Zuppinger

Received: 19 October 2011 / Accepted: 25 June 2012 / Published online: 4 August 2012

Abstract The clinical use of anthracyclines in cancer therapy is limited by dose-dependent cardiotoxicity that involves cardiomyocyte injury and death. We have tested the hypothesis that anthracyclines affect protein degradation pathways in adult cardiomyocytes. To this aim, we assessed the effects of doxorubicin (Doxo) on apoptosis, autophagy and the proteasome/ubiquitin system in long-term cultured adult rat cardiomyocytes. Accumulation of poly-ubiquitinated proteins, increase of cathepsin-D-positive lysosomes and myofibrillar degradation were observed in Doxo-treated cardiomyocytes. Chymotrypsin-like activity of the proteasome was initially increased and then inhibited by Doxo over a time-course of 48 h. Proteasome 20S proteins were down-regulated by higher doses of Doxo. The expression of MURF-1, an ubiquitin-ligase specifically targeting myofibrillar proteins, was suppressed by Doxo at all concentrations measured. Microtubule-associated protein 1 light chain 3B (LC3)-positive punctae and both LC3-I and -II proteins were induced by Doxo in a dose-dependent manner, as confirmed by using lentiviral expression of green fluorescence protein bound to LC3 and live imaging. The lysosomotropic drug chloroquine led to autophagosome accumulation, which increased with concomitant Doxo treatment indicating enhanced autophagic flux. We conclude that Doxo causes a downregulation of the protein degradation machinery of cardiomyocytes with a resulting accumulation of poly-ubiquitinated proteins and autophagosomes. Although autophagy is initially stimulated as a compensatory response to cytotoxic stress, it is followed by apoptosis and necrosis at higher doses and longer exposure times. This mechanism might contribute to the late cardiotoxicity of anthracyclines by accelerated aging of the postmitotic adult cardiomyocytes and to the susceptibility of the aging heart to anthracycline cancer therapy.

Keywords Autophagy · Apoptosis · Doxorubicin · Cardiomyocytes · Proteasome · Rat (Wistar, adult male)

Introduction

The anthracycline doxorubicin (Doxo) is a well-established drug used clinically in cytotoxic antitumor therapy for several types of cancers. Potentially life-threatening cardiotoxicity remains a problem with the anthracyclines and limits the cumulative dose that can be administered safely (Singal and Iliskovic 1998). Several studies have evaluated the incidence and risk of early clinical cardiotoxicity, as characterized by arrhythmias, a reversible depression of contractile function and the more common late cardiotoxicity (Bristow et al. 1984; Steinherz et al. 1991). Cardiac abnormalities have been observed years after treatment and seem to occur independently of whether cardiac problems appeared during initial therapy (Goorin et al. 1990). The long-term effect of Doxo on the cardiovascular system is

Electronic supplementary material The online version of this article (doi:10.1007/s00441-012-1475-8) contains supplementary material, which is available to authorized users.

This work was supported by a Swiss National Science Foundation grant to C.Z. (3100A0-120664) and research grants from Hoffmann La-Roche to T.M.S.

P. Dimitrakis · M.-I. Romay-Ogando · F. Timolati · T. M. Suter · C. Zuppinger
Cardiology, Swiss Cardiovascular Center Bern,
Bern University Hospital and University of Bern,
Bern, Switzerland

C. Zuppinger (✉)
Cardiology, Department of Clinical Research MEM E808,
Bern University Hospital,
Murtenstrasse 35,
3010 Bern, Switzerland
e-mail: christian.zuppinger@dkf.unibe.ch

especially evident in young patients: 71% of children that have been followed up for >15 years after doxorubicin therapy develop cardiotoxicity (Steinherz et al. 1991). The mechanisms of the cardiotoxicity of anthracyclines appearing many years after treatment are not known. A loss of cardiomyocytes by cell death shortly after the first anthracycline treatment could be a likely cause but fails to explain cases in which no cardiotoxicity was noticed initially; indeed, apoptosis was not demonstrated at lower cumulative doses of doxorubicin in experimental models (Zhang et al. 1996). Further suggested mechanisms include the impairment of cardiac progenitor cell function in juvenile hearts by anthracyclines and persisting damage to mitochondrial DNA, which would represent the basis of a self-perpetuating mitochondrial dysfunction (Huang et al. 2010; Lebrecht and Walker 2007). Elderly patients are generally more susceptible to anthracycline cardiotoxicity because of comorbidities, such as hypertension, diabetes and limited cardiac reserve (Aapro et al. 2011). On the other hand, postmitotic and long-living cells such as cardiomyocytes accumulate protein aggregates and defective mitochondria with age, which could accelerate cell death under stress conditions. A common observation illustrating normal age-related changes in the myocardium is the augmentation of a non-degradable yellow-brown pigment composed of lipid and oxidized protein residues, the so-called lipofuscin, in cardiomyocytes of elderly people (De Meyer et al. 2010; Powell et al. 2005). Lipofuscin generation is enhanced by reactive oxygen species (ROS). Oxidative stress is also thought to be a general problem with anthracyclines, since the quinone moiety of the molecule acts as a catalyst for the formation of ROS (Doroshow and Davies 1986). In cardiomyocytes, increased levels of intracellular calcium and ROS can trigger the activation of proteases that cause damage to myofibrillar proteins, e.g., titin and lead to contractile dysfunction (Lim et al. 2004; Timolati et al. 2009). The ubiquitin/proteasome system represents the main degradation pathway involved in the removal of oxidatively modified proteins (Grune et al. 2004), whereas (macro-) autophagy is generally considered a proteasome-independent catabolic mechanism for bulk degradation and routine turnover of larger cell constituents (Glick et al. 2010; Xie et al. 2011). Previous studies have shown an important role of the ubiquitin/proteasome in the heart challenged by anthracyclines, which have been proposed to induce a potentially harmful over-activity of this protein degradation system in cardiomyocytes (Kumarapeli et al. 2005; Ranek and Wang 2009).

We have tested the hypothesis that anthracycline cancer therapy modulates several protein degradation pathways in adult cardiomyocytes. We have found that Doxo applied for 48 h causes dose-dependent effects, namely myofibrillar disarray at lower doses and a downregulation of the proteasome-ubiquitin system at higher doses with the resulting accumulation of poly-ubiquitinated proteins, cathepsin-D-positive lysosomes and autophagosomes. Whereas proteasome activity and autophagy are stimulated initially as a compensatory response to cytotoxic stress and the accumulation of oxidized proteins, this is followed by apoptosis and necrosis at higher doses and longer exposure times.

Materials and methods

Isolation of adult rat ventricular cardiomyocytes

Adult (280–350 g) male Wistar rats from an in-house breeding facility were killed by pentobarbital (Abbott Laboratories) injection. The heart was excised and the aorta was cannulated and retrograde perfused at 90 cm H_2O pressure. Isolation of calcium-tolerant adult rat ventricular myocytes (ARVM) was achieved according to previously published methods (Kondo et al. 1998). The cells were plated onto laminin-coated (10 μg/ml mouse laminin, Invitrogen) cell culture dishes (Nunc) and maintained in serum-containing medium for the entire culture period. Culture medium was based on M-199 (Amimed) and additionally contained 20 mM creatine (Sigma), 1% 100 U/ml penicillin/streptomycin (Invitrogen), 20% preselected fetal calf serum (PAA Laboratories) and 10 μM cytosine arabinoside (Sigma). All experiments were carried out according to the Swiss animal protection law and with the permission of the State Veterinary Office. The investigation conformed to the "Guide for the Care and Use of Laboratory Animals" published by the US National Institutes of Health.

Immunocytochemistry and fluorescence microscopy

Cell cultures were washed with phosphate-buffered saline (PBS), then fixed with 3% para-formaldehyde in PBS for 15 min, permeabilized with 0.2% Triton-X100 (Sigma) in PBS for 10 min or with ice-cold methanol for 5 min, incubated for 30 min with bovine serum albumin (Sigma) at 1 mg/ml in PBS at room temperature, incubated overnight with primary antibodies at 4°C, washed three times with PBS and incubated for 1 h with secondary antibodies coupled to Alexa fluorescent dyes (Invitrogen). Preparations were examined either by using an inverted microscope (Leitz DM IL) and a 40× oil immersion lens (NA 1.3, Olympus; see below) or on a Zeiss LSM 5 Exciter confocal microscope using 40× or 63× Zeiss oil immersion lenses (see below and Fig. S1). Monoclonal antibodies to myosin heavy chain clone A4.1025 were obtained from Millipore (catalog no. 05-716). Actin was detected by using polyclonal antibodies to all-actin (A2066, Sigma). Anti-myomesin mouse monoclonal antibodies (clone B4) were a gift from J.C. Perriard, ETH-Zurich, Switzerland. Monoclonal antibodies, namely clone FK1 to poly-ubiquitinated protein

adducts, were obtained from Biomol. This antibody recognizes K29-, K48- and K63-linked polyubiquitinated proteins but not mono-ubiquitinated proteins or free ubiquitin (Fujimuro and Yokosawa 2005). Rabbit polyclonal antibodies to subunits of the 20-S-proteasome core (catalog no. PW8155) were from Biomol. Antibodies for Atg8/microtubule-associated protein 1 light chain 3B (LC3) were from Abcam (polyclonal, catalog no. ab58610) or from nanotools (monoclonal, clone 2 G6). For immunocytochemistry, the anti-LC3 clone 2 G6 was used throughout. Antibodies to rat cathepsin-D (clone R20) were from Santa Cruz Biotechnology. Monoclonal antibodies to titin I-band (clone 9D10) were obtained from the Development Studies Hybridoma Bank at the University of Iowa and polyclonal antibodies to the titin M-line domain (M8) were a gift from Mathias Gautel, King's College, London. Secondary antibodies for immunocytochemistry were conjugated with Alexa fluorescent dyes (Invitrogen).

Pharmacologic treatments

Doxorubicin-hydrochloride (Doxo; Sigma) was dissolved in water. Lactacystin and chloroquine were obtained from Calbiochem (Merck group) and were dissolved in dimethylsufoxide (DMSO).

Cell death and viability assays

TUNEL assay TUNEL (terminal deoxyribonucleotidyl-transferase mediated D-uridine 5′-triphosphate nick-end labeling) assay was performed according to the manufacturers instructions ("In situ cell death detection kit AP", Roche Applied Science), with the exception of prolonged permeabilization. Incubation with DNAse-I (Sigma) was used as a positive control for DNA nick labeling. In order to avoid interference of red-fluorescent nuclei in the counting of TUNEL-positive cells by fluorescence microscopy after Doxo treatment, conversion to an alkaline-phosphatase-based detection system was performed (5-bromo-4-chloro-3-indolyl-phosphate/nitroblue tetrazolium substrate, Sigma).

Western blot analysis

Cells were quickly washed with ice-cold PBS and lysed by using modified RIPA lysis buffer (1% NP-40, 0.2% SDS, 0.25% deoxycholic acid, 50 mM TRIS-HCl pH 7.4, 1 mM EDTA, 150 mM NaCl, 1 mM NaF, 1 μg/ml leupeptin, 1 mM phenylmethane sulfonylfluoride, 1 mM sodium orthovanadate, 2 μg/ml pepstatin, 1 μg/ml aprotinin). For the analysis of poly-ubiquitinated proteins by Western blot (see below), cells were lysed in cold lysis buffer containing 3.7 M urea, 134.6 mM TRIS, 5.4% SDS, 2.3% NP-40, 4.45% beta-mercaptoethanol, 4% glycerol, 6 mg/100 ml bromophenol blue. Cell lysates were boiled with a loading buffer containing 3.3% glycerin, 1% SDS 20 mM TRIS pH 6.8, 23 mM β-mercaptoethanol (freshly added) and 0.4 mg/ml bromophenolblue). Proteins were separated by SDS-polyacrylamide gel electrophoresis (SDS-PAGE) by using precast 4%–20% gradient gels (Lonza, Invitrogen) and blotted to nitrocellulose (Whatman) or polyvinylidene difluoride membranes with low autofluorescence (Millipore). Immunodetection was carried out after the blocking of the membrane in 5% milk or gelatin in TTBS (20 mM TRIS base pH 7.5, 150 mM NaCl, 0.05% Tween-20). Signals from polyclonal antibodies to all-actin (A2066, Sigma) or monoclonal antibodies to sarcomeric actin (A2172, Sigma) were used as a reference for normalizing the protein amount in each lane. For the visualization of signals, a LiCor Odyssey infra-red imaging system was used with secondary antibodies coupled to IRDye fluorescent dyes (LiCor).

Proteasome activity

The chymotrypsin-like activity of the proteasome was measured by monitoring the cleavage of the fluorogenic substrate Suc-Leu-Leu-Val-Tyr-7-amino-4-methylcoumarin (Chemicon/Millipore; catalog no. APT280). The irreversible proteasome inhibitor lactacystin was used as a negative control. DMSO, the solvent used for lactacystin treatment, was included in control cultures. Freshly made protein extracts from ARVM containing equal amounts of protein measured by the Bradford assay (BioRad) in a photometer were incubated for 60 min with assay buffer and substrate at 37 °C in the dark. The lysis buffer contained 50 mM HEPES (pH 7.5), 5 mM EDTA, 150 mM NaCl, 2 mM ATP (freshly added) and 1% Triton X-100. The amount of free 7-amino-4-methylcoumarin (AMC) as a measure of the chymotrypsin-like activity of the 20S proteasome was assessed in a Safire microplate fluorescence reader (Tecan).

RNA isolation and real-time polymerase chain reaction

RNA isolation from cell cultures was performed with a kit from Qiagene (RNeasy fibrous tissue kit). RNA quality was tested by measuring the ratio 260/280 nm in a UV-photometer. Reverse transcription was performed by using the iScript cDNA synthesis kit (BioRad). Primers purified by high-pressure liquid chromatography were ordered from TIB Molbiol. Gene sequences were retrieved from the National Center for Biotechnology Information (NCBI) database. Primers were designed by using the software "Primer 3" (Whitehead Institute for Biomedical Research) and tested for specificity with BLAST (NCBI) searches against rat genome. Real time polymerase chain reactions (PCRs) were

performed with the iCycler (Biorad) and iQ SYBR Green mix including i*Taq*-polymerase. For standard PCR amplification, the Ex TAq and additional chemicals from TaKaRa Bio were employed. The geometric mean of the housekeeping genes 18S and hypoxanthine phosphoribosyl-transferase (HPRT) was used for normalization. The primer for MURF-1 (muscle-specific RING finger protein 1) was chosen according to previously published sequences (Adams et al. 2007). Primers are listed as follows: 18s, X01117, forward, gtaacccgttgaaccccatt, reverse, ccatccaatcggtagtagcg, HPRT, NM012583, forward tgtggccagtaaagaactagca, reverse gacaatctacctgacggtaggc, MURF-1, NM080903.1 forward tccaaggacagaagactgaact, reverse tggaagcttctacaatgctctt.

Lentiviral expression of green fluorescence protein bound to LC3 and live imaging

Cardiomyocytes were cultured on laminin-coated glass bottom dishes (Greiner bio-one) in standard medium and transduced with lentiviral particles at a multiplicity of infection of 50. Lentiviral particles carrying a construct of TagGFP2-LC3 driven by the elongation factor-1 promoter (Millipore LentiBrite) were applied for 24 h, the medium was changed and the pharmacological treatment was started after another 24 h. Live images were obtained by using an inverted microscope (Leitz DM IL), Olympus 40× objective and a Nikon Coolpix990 camera.

Statistics

All values are expressed as mean±SEM. Statistical analysis of differences observed between the groups was performed by Student's unpaired *t*-tests or by analysis of variance, followed by Bonferroni's repeated measurement comparisons, when appropriate. Statistical significance was accepted at the level of $P<0.05$.

Results

Doxo-induced changes of myofibrillar structure

ARVM in long-term culture in the presence of fetal calf serum assume a polygonal shape, form intercalated disc-like structures and myofibrils and resume contractile activity (Eppenberger and Zuppinger 1999). Untreated cardiomyocytes showed a well-developed non-sarcomeric cytoskeleton and myofibrils after 14 days in culture, as demonstrated by immunocytochemistry with antibodies for all-actin and myosin heavy chains (Fig. 1a). Treatment with 10 μM Doxo for 48 h resulted in a clumping of cytoskeletal elements. The sarcomeric striation of myofibrils disappeared to a large extent and the overall staining for myosin was reduced (Fig. 1b). At this dose of Doxo, changes in the morphology of nuclei became apparent and 4,6-diamidino-2-phenylindole (DAPI) labeling of nucleic acids was less homogeneous than that in controls. Potential mechanisms of the observed cytoskeletal damage after Doxo treatment involving increased cytoplasmic calcium, activation of calpain-I and the cleavage of titin have been investigated previously in this model (Lim et al. 2004; Timolati et al. 2009). A group of Doxo-treated ARVM presumably showing different stages of cytoskeletal degradation is shown in the electronic supplementary material (Fig. S1a-a'').

DNA degradation

For measuring DNA degradation as a marker of apoptosis, we used the TUNEL assay, with DNase serving as a positive control (Fig. 2). A significant increase in the frequency of TUNEL-positive cardiomyocytes was observed at 10 μM and higher doses of Doxo for 48 h. Other viability parameters such as mitochondrial respiration and plasma membrane integrity have demonstrated a dose-dependent increase of cell death with doses of >10 μM/48 h in previous studies in our laboratory (Timolati et al. 2009).

Doxo induces polyubiquitin aggregates and cathepsin-D-positive lysosomes

Granular cytoplasmic inclusions of ubiquitinated proteins, also called aggresomes, have been observed in cardiac tissue taken from patients suffering from ischemic cardiomyopathy or dilated cardiomyopathy (Knaapen et al. 2001) and in pressure-overload hypertrophy and after glucose deprivation in experimental models (Marambio et al. 2010; Tannous et al. 2008). We tested the integrity of myofibrils by using the M-line protein myomesin as a marker and examined the localization and amount of polyubiquitinated proteins in the same cells treated with increasing doses of Doxo (Fig. 3). The antibody FK1 recognizes K29-, K48- and K63-linked polyubiquitinated proteins but not mono-ubiquitinated proteins or free ubiquitin (Fujimuro and Yokosawa 2005). ARVM were cultured until day 12 and then treated with 1 μM (Fig. 3b, b') or 10 μM Doxo (Fig. 3c, c'). Polyubiquitin labeling was found as diffuse staining in the cytoplasm of untreated ARVM with intact myofibrils (Fig. 3a, a'). Occasionally, the signals from the anti-polyubiquitin antibodies showed a sarcomere-like striated pattern in untreated ARVM (not shown). Degradation of myofibrils with concomitant accumulation of polyubiquitinated proteins occurred even at the sub-apoptotic dose of 1 μM Doxo (Fig. 3b, b'). Signals from aggregates of polyubiquitinated proteins and granular aggregates of myomesin were colocalized in Doxo-treated ARVM (Electronic Supplementary Material, Fig. S1b). The distribution of large

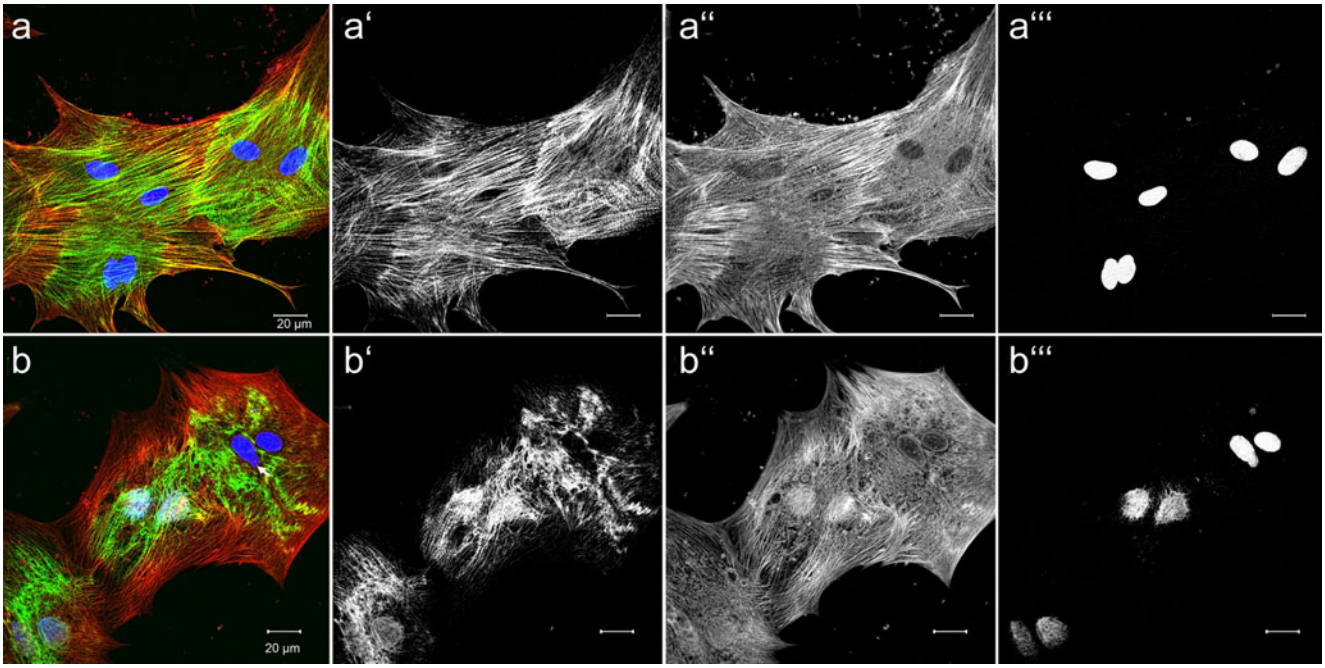

Fig. 1 Doxorubicin (Doxo) induces cytoskeleton changes with loss of myofibrils and clumping of the non-sarcomeric cytoskeleton. **a** Untreated cells. **b** Adult rat ventricular myocytes (ARVM) were cultured for 12 days and then treated for 48 h with 10 μM Doxo. Myofibrils were labeled with antibodies to anti-myosin heavy chain (*green*) and actin filaments were labeled with anti-all-actin antibodies (*red*); nuclei were stained with DAPI (*blue*)

inclusions of polyubiquitinated proteins was heterogeneous in cell populations. Cells with large aggresomes always showed myofibrillar changes but not vice-versa. In Doxo-treated ARVM, red fluorescence in the nuclei was observed indicating the accumulation of anthracycline. Nuclear Doxo fluorescence was usually seen in paraformaldehyde-fixed cells (Fig. 3b/b', c/c') but not in methanol-fixed ARVM (Fig. 3e). The aspartic proteases of the cathepsin family participate in maintaining the homeostasis of the metabolism of the cell by the bulk-degradation of aggregated proteins and entire organelles (Gevers 1984). Cathepsin-D-positive vesicles were found in untreated ARVM but increased in number and size with Doxo treatment, especially in the perinuclear area (10 μM/48 h; Fig. 3d, e).

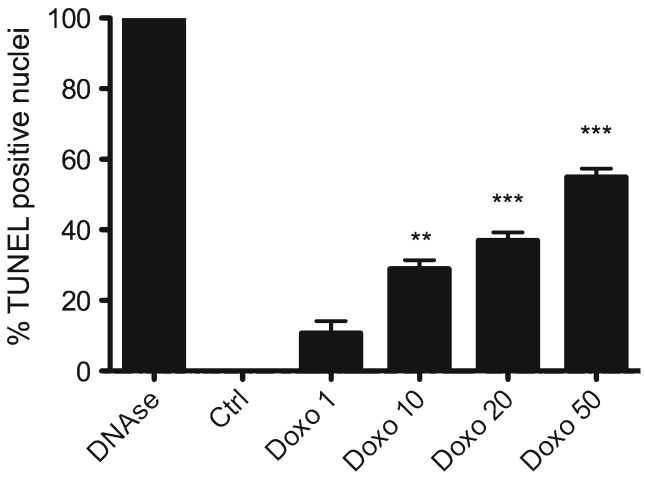

Fig. 2 Doxo induces DNA fragmentation in ARVM in a dose-dependent manner (*Ctrl* control). ARVM were treated for 48 h before fixation and terminal deoxyribonucleotidyl-transferase mediated D-uridine 5′-triphosphate nick-end labeling (*TUNEL*) assay. $^{**}P<0.01$, $^{***}P<0.001$, $n=4$

Modulation of the ubiquitin/proteasome system by Doxo

We assessed the state of the ubiquitin-proteasome system in ARVM treated with Doxo (Fig. 4). The 20S proteasome core components were found in a cross-striated pattern and at intercalated disc-like structures in untreated ARVM (Fig. 4a). A similar pattern was detected for ubiquitin in cardiomyocytes (not shown). The observed localization of the ubiquitin/proteasome system in ARVM in long-term culture was in agreement with previous reports of its localization in ventricular tissue in vivo (Hilenski et al. 1992). The same 20S proteasome core proteins were analyzed by using Western blot after Doxo treatment for 48 h, normalized to sarcomeric actin (Fig. 4b). No significant change occurred at lower concentrations of Doxo but a significant decrease took place at concentrations associated with irreversible cell death. We then assessed the chymotrypsin-like activity of the proteasome with an assay measuring the degradation of the sequence Suc-Leu-Leu-Val-Tyr in cellular lysates (Fig. 4c, d). The same amount of total protein, as measured by the Bradford assay, was used for each

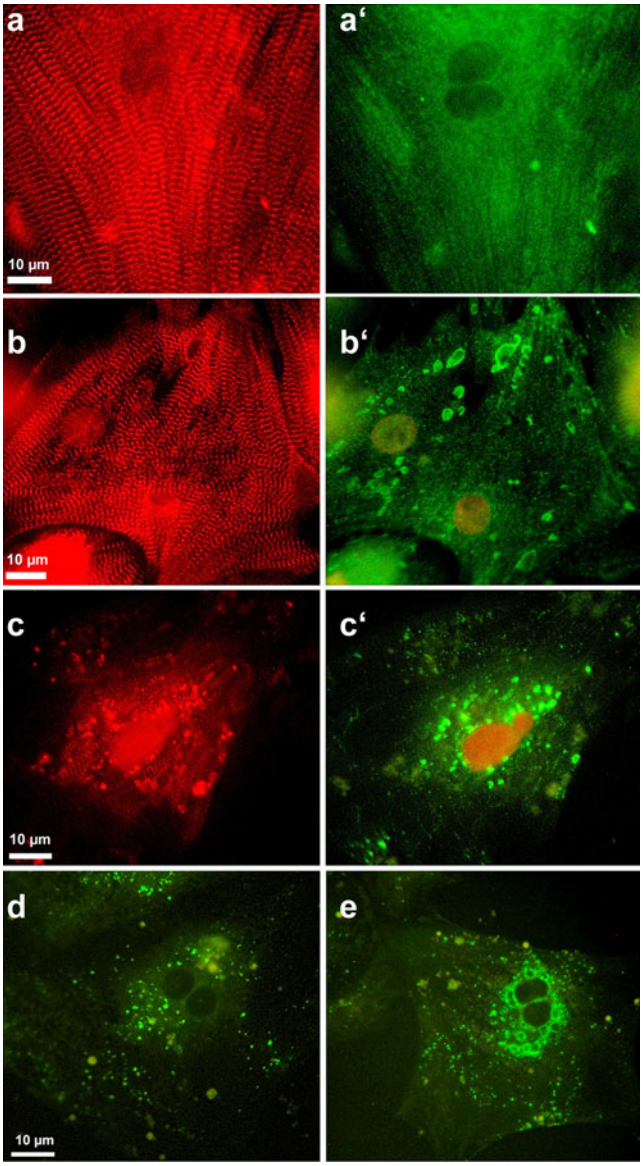

Fig. 3 Accumulation of aggresomes marked by polyubiquitinated proteins, loss of myofibrils and increase of cathepsin-D-positive lysosomes after Doxo treatment. **a/a'-c/c'** ARVM were treated with Doxo (**a/a'** untreated, **b/b'** 1 µM, **c/c'** 10 µM) for 48 h and then immunostained for myomesin (*red*) or polyubiquitinated proteins (*green*). **d**, **e** ARVM were immunostained for cathepsin-D (*green*). **d** Untreated. **e** 10 µM Doxo

condition. In the first assay, we measured the activity in a short-term treatment with either 1 or 50 µM Doxo and expressed the result as percent of the activity in an untreated sample at the same time point (Fig. 4c). The lower Doxo concentration resulted in a generally elevated activity from the beginning, which slowly declined after 18 h. The high dose increased the activity until 3 h and then the activity declined rapidly. These results were confirmed in a second assay in which the activity was measured (shown as absolute values) after 48 h (Fig. 4d). The measured activity was unchanged below 10 µM Doxo and then declined rapidly at higher concentrations. The irreversible proteasome inhibitor lactacystin served as a negative control. The results from the proteasome Western blots (Fig. 4b) indicated that not only the activity but also the proteasome itself was affected in the cells treated with extremely high concentrations of Doxo. We then assessed polyubiquitinated proteins by Western blot after Doxo treatment in the range of 1–20 µM for 48 h (Fig. 4e). The most intense labeling by the FK1 antibody was observed with 10 µM Doxo treatment in the molecular weight range above 100 kDa. Longer exposure times resulted in a smear over the entire weight range (not shown). Apart from the proteasome machinery itself, a series of enzymes play a crucial role in the ubiquitination of target proteins and therefore in protein turnover. The specificity of the ubiquitination lies primarily with the ubiquitin E3 ligases and MuRFs, especially MURF-1, have been identified as E3 ligases targeting myofibrillar proteins such as actin, titin and others in skeletal muscle and in the myocardium (Gregorio et al. 2005; Mrosek et al. 2007; Polge et al. 2011). We have measured the expression of MURF-1 by real time PCR in ARVM after Doxo treatment for 48 h (Fig. 4f). MURF-1 mRNA was significantly reduced by Doxo at all concentrations measured.

Doxo increases autophagy in ARVM

LC3, the mammalian homolog of yeast Atg8, was originally identified as a binding partner of microtubule-associated proteins, until its role during the formation of autophagosomal membranes was discovered. Cytosolic LC3-I undergoes conjugation to highly lipophilic phosphatidylethanolamine by Atg7, Atg3 and the Atg12-Atg5/Atg16 complex to form the autophagosome-associated LC3-II, which runs differently from LC3-I in SDS-PAGE and serves as a marker of autophagosomes in immunofluorescence microscopy (Kabeya et al. 2000; Mizushima et al. 2001). The distribution and appearance of LC3 in untreated ARVM and in cells exposed to 10 µM Doxo for 48 h is demonstrated in Fig. 5a, b, respectively. LC3-positive puncta, often single spots on a low cytoplasmic background, were occasionally also observed in untreated cells; however, the number of LC-positive vesicles after Doxo treatment increased, as did the cytoplasmic staining for LC3. Interestingly, filamentous structures reminiscent of microtubules were observed in some of the Doxo-treated ARVM showing an increase of puncta and cytoplasmic staining (Fig. 5b). We then assessed LC3-I/II by Western blotting (Fig. 5c). Doxo treatment for 48 h generally increased LC3. However, different antibodies showed distinctive affinities to LC3-I/II: polyclonal antibody ab58610 mainly recognized LC3-I in ARVM, whereas monoclonal antibody clone 2G6 demonstrated the increase of LC3-II in the cells. Densitometry of signals from the

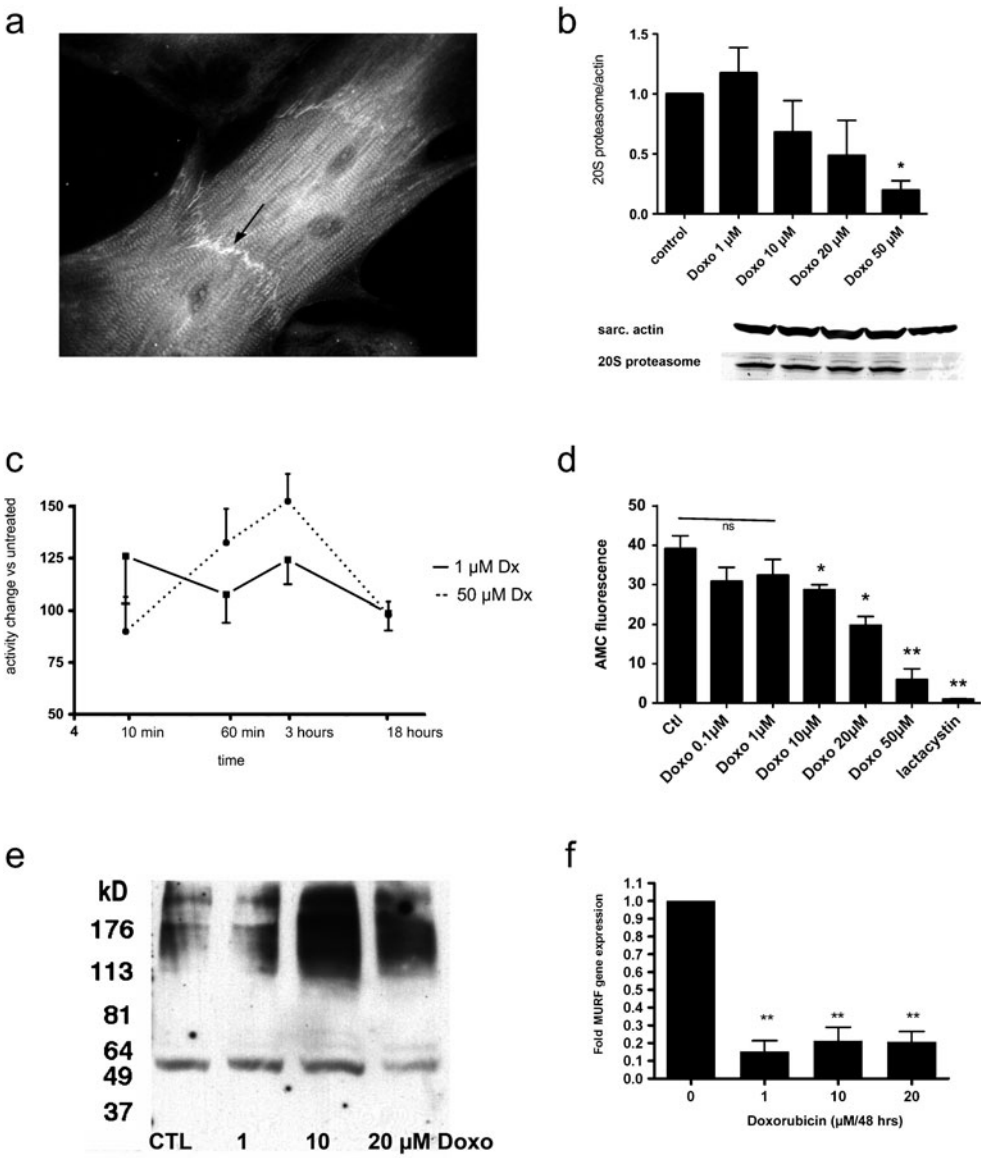

Fig. 4 Effects of Doxo on the proteasome/ubiquitin system in ARVM. **a** Subcellular localization of the 20S proteasome core components in untreated ARVM. Labeling was mainly found in a cross-striated pattern and at the intercalated disc-like structures (*black arrow*). **b** Densitometry and representative Western blot for the 20S proteasome normalized to sarcomeric actin. ARVM were treated for 48 h with the indicated Doxo doses. **c** Proteasome activity in lysates was measured after the indicated times for 1 and 50 μM Doxo. Results are shown normalized to untreated cells of the same age. **d** Proteasome activity after treatment with the indicated Doxo doses for 48 h. The irreversible proteasome inhibitor lactacystin was used as a negative control (*ns* not significant). **e** Western blot for polyubiquitinated proteins in ARVM treated with the indicated Doxo doses for 48 h (*CTL* control). **f** Gene expression of MURF-1 was normalized to the expression of two house-keeping genes and to untreated ARVM. **P*<0.05, ***P*<0.01, *n*=4

antibody 2G6 normalized to all-actin showed a significant increase of LC3-II at 20 μM Doxo (Fig. 5d). Additional experiments examining green fluorescence protein (GFP)-LC3 expression after lentiviral transduction of cardiomyocytes demonstrated LC3 localisation in live cells without possible artifacts being introduced by fixation or the use of antibodies (Fig. 5f–h). GFP-LC3 was observed in puncta but mainly displayed a diffuse cytosolic distribution (Fig. 5f). After treatment with Doxo (Fig. 5g), no diffuse fluorescence was observed but rather GFP-LC3 puncta similar to the immunofluorescence results. Treatment with chloroquine, an inhibitor of autophagosome/lysosome fusion, led to large cytosolic vacuoles, which appeared outlined by the GFP-LC3 signal in the live cells (Fig. 5h). Increased LC3-II levels might have been associated with either enhanced autophagosome synthesis or reduced autophagosome turnover, perhaps attributable to delayed trafficking to the lysosomes, reduced fusion between compartments, or impaired lysosomal proteolytic activity (Barth et al. 2010). We therefore sought a method to discern these two situations. The inhibition of autolysosome function by using an inhibitor such as chloroquine or bafilomycin leads to an accumulation of LC3-positive autophagosomes as a sign of efficient autophagic flux, whereas the absence of such an accumulation, either over time or in combination with a hypothetical modulator of autophagy, indicates a failure of the autophagic machinery earlier in the process. We used chloroquine for the purpose of elucidating changes of autophagic flux caused by Doxo treatment in ARVM (Fig. 6). Cells were immunostained for LC3 by using antibody clone 2G6 and for polyubiquitinated proteins. Chloroquine alone at 10 μM for 48 h led to an increase and homogeneous distribution of

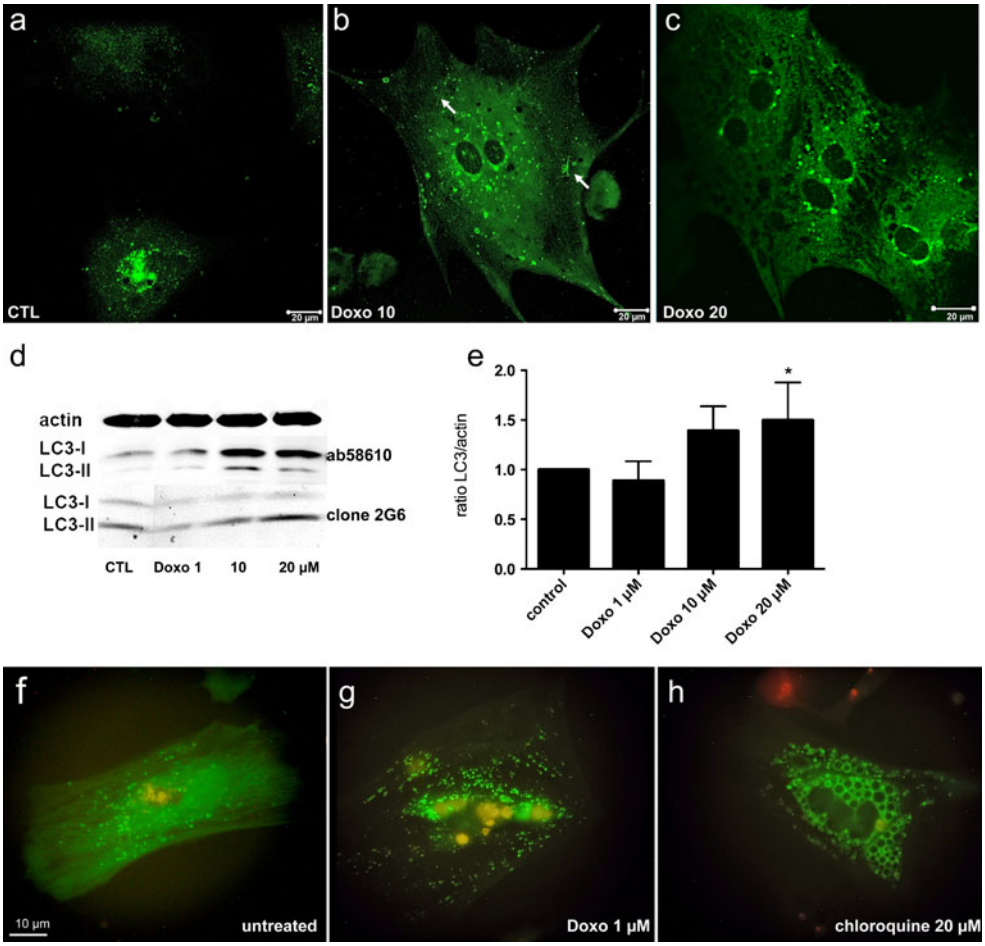

Fig. 5 Doxo induces LC3-I/II- and LC3-positive punctae in ARVM. **a–c** ARVM were cultured for 12 days and then treated with 0, 10, or 20 μM Doxo for 48 h and immunostained for LC3. Note the increased LC3-positive punctae, diffuse staining and occasional filamentous structures (*white arrows* in **b**). **d** Representative Western blots for Doxo-treated ARVM tested with two different antibodies showing differential labeling of LC3-I/II. **e** Densitometry for LC3 with antibody clone 2 G6. **f–h** Live cardiomyocytes expressing GFP-LC3 after lentiviral transduction and pharmacologic treatment for 48 h. **f** Untreated cells. **g** Doxo at 1 μM. **h** Chloroquine at 20 μM

LC3 puncta. Polyubiquitinated proteins were found in most cells in the form of smaller aggregates that co-localized with the autophagosome marker LC3 but were overall not significantly increased (Fig. 6a/a'). The combination of chloroquine at 20 μM and Doxo at 10 and 20 μM showed a dose-dependent increase of LC3 and aggregates of polyubiquitinated proteins that increasingly colocalized with increased Doxo concentration (Fig. 6b, c)

Discussion

We report the effects of anthracyclines on protein degradation systems and cell death in cultured adult cardiomyocytes. We decided to use cells from adult animals for this study, although technically more challenging, because differences in cell cycle activity and gene expression between immature and differentiated cells are common. Cell models showing active proliferation might respond differently to cancer therapies by stalled mitosis and subsequent cell death, which is not necessarily the case in terminally differentiated cells. This basic principle is illustrated by the action of antimetabolites and proliferation inhibitors such as Ara-C that are sometimes added to primary cardiomyocyte cultures for limiting the growth of non-myocytes after isolation. Occasionally, differences between neonatal and adult cardiomyocytes have been investigated in detail and significant dissimilarities have been noted, for instance, for calcium handling and the regulation of Doxo-induced apoptosis (Konorev et al. 2008; Poindexter et al. 2001). An overall higher sensitivity of neonatal cardiomyocytes for anthracycline-induced apoptosis has been noted in a previous study: neonatal cardiomyocytes exposed to 0.5 μM doxorubicin for 24 h exhibit a nearly three-fold increase of apoptotic cells as quantified by flow cytometry, whereas adult cardiomyocytes do not show cell death under this condition (Lim et al. 2004). Anthracyclines have been reported to reach peak concentrations in plasma of up to 5 μM and the values are generally in the range of 1-2 μM in patients after bolus injection (Gewirtz 1999). For in situ models with a short life time and thus short time of drug persistence, such as the isolated perfused heart, muscle strips, or isolated mitochondria, often supraclinical Doxo concentrations up to several hundreds of micromoles have been applied (Tokarska-Schlattner et al. 2006). Although cell death in cardiomyocytes has been reported in

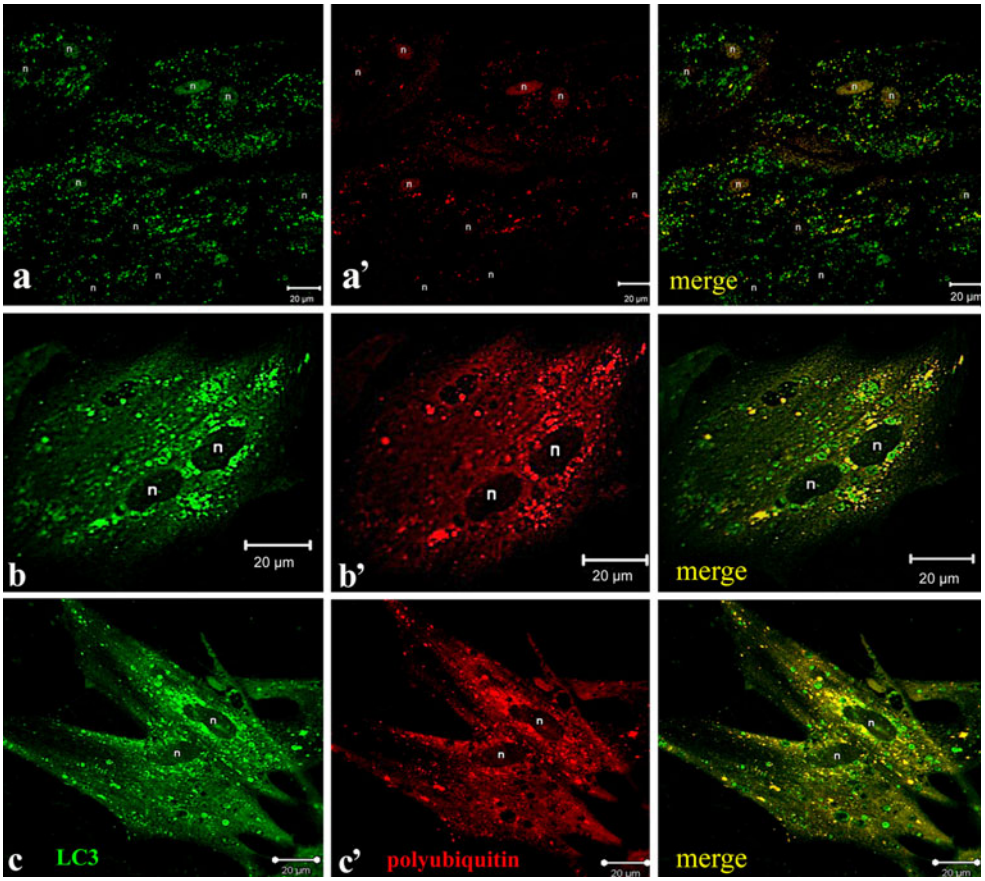

Fig. 6 Chloroquine and Doxo increase autophagosome accumulation indicating higher autophagic flux in treated ARVM. ARVM were treated with chloroquine 20 µM and Doxo 1 µM in **a/a'**, with chloroquine 20 µM and Doxo 10 µM in **b/b'** and with Doxo 20 µM and chloroquine 20 µM for 48 h in **c/c'**. Cells were then fixed and immunostained for LC3 (*green*) and for polyubiquitinated proteins (*red*) and single optical sections were taken by confocal microscopy. Co-localizing signals appear in *yellow* in the merged images

many different laboratory models (Singal and Iliskovic 1998), the use of extremely high concentrations in cell culture experiments might lead to an overestimation of cell death as a mechanism of anthracycline-induced cardiotoxicity. Therefore, we have chosen a range of concentrations, for most experiments in this study, starting from below the above-mentioned numbers found in plasma up to supraclinical concentrations applied for a relatively long period of time (usually 48 h) in culture.

A larger body of literature is available describing the cardiotoxic mechanisms of anthracyclines at the level of the muscle cell (for a review, see Sawyer et al. 2010). Recently, other stress-related pathways than irreversible cell death have been investigated, in the hope that ways can be found to repair and rescue myocardial tissue. Our results demonstrate that LC3-positive puncta and total LC3 increase as a result of anthracycline treatment in cultured ARVM. This result has been confirmed by Western blotting for LC3 by using different antibodies. To test whether the choice of antibodies or the fixation of the cells causes artifacts in the localization of LC3-positive puncta, we have used a GFP-LC3 construct, lentiviral transduction and live imaging of cardiomyocytes. Although this method is also not devoid of possible distorting effects, such as the formation of GFP-aggregates at high expression levels or effects of the viral vectors (Klionsky et al. 2008), the observed alterations between the control situation and anthracycline-treated cells, such as the observed switch from a diffuse cytosolic GFP-LC3 distribution to a punctate one, demonstrates the induction of autophagy by Doxo in these cells. Additionally, cathepsin-D-positive lysosomes are increasingly found with a perinuclear distribution and the lysosomotropic drug chloroquine leads to autophagosome accumulation, which increases with concomitant Doxo treatment indicating enhanced autophagic flux.

Generally, the functional role of enhanced autophagy in the heart is still unclear and studies have reported conflicting results. Should autophagy be regarded as a protective mechanism or as a process contributing to disease progression? Earlier studies have described autophagy-related changes in human failing hearts as a form of cell death (Hein et al. 2003; Knaapen et al. 2001; Kostin et al. 2003). Current evidence indicates that autophagic activity under physiological conditions is important for cellular homeostasis, whereas excessive autophagy is detrimental (Nishida et al. 2009; Kobayashi et al. 2010). Autophagy predominantly functions as a pro-survival pathway during nutrient deprivation and other forms of cellular stress, as has been demonstrated in a number of model systems and in rare human diseases. However, when autophagy is rigorously activated, the

autophagic machinery might also be used for self-destruction (Nemchenko et al. 2011). Hence, when autophagic cell death occurs in cardiac cells, it might contribute to the progress of heart failure. On the other hand, if the rate of autophagy declines with age, this progressively leads to the inability to process and remove accumulated "waste", such as lipofuscin or the polyubiquitinated protein aggregates that have been found after Doxo treatment in our experiments. The progress of these changes results in enhanced oxidative stress, decreased ATP production, collapse of the cellular catabolic machinery and hence, necrosis or apoptosis. By contrast, in load-induced heart failure, the extent of autophagic flux can rise to maladaptive levels (Zhu et al. 2007). Accordingly, the development of therapies that up-regulate the repair qualities of the autophagic process and down-regulate the cell death aspects would be of great value in the treatment of heart failure (De Meyer et al. 2010). In this context, we consider it of interest to compare features of normal aging of the myocardial tissue with effects of Doxo-induced cardiotoxicity. Protein aggregation seems to be a common feature of physiological aging. Even greater cell damage indicated by the loss of myofibrils, the swelling of mitochondria and the accumulation of lipofuscin granules is seen in an older adriamycin-treated group of animals (Weinberg and Singal 1987). Thus, the loss of proteasome function might impair the ability of myocytes to mount an appropriate response to stress, thereby enhancing the susceptibility of the aging heart to cardiovascular disease (Bulteau et al. 2002). The combination of these factors means that the natural decline in cardiac reserve is accelerated by anthracycline-induced cardiotoxicity.

The ubiquitin-proteasome system plays an important role in the heart for the continuous degradation and removal of oxidized or misfolded proteins (for reviews, see Powell 2006; Wang et al. 2008). In heart failure, a disturbed balance between a high rate of ubiquitination and inadequate degradation of ubiquitin/protein conjugates might finally contribute to autophagic cell death and the loss of cardiomyocytes in the tissue (Kostin et al. 2003). In this study, we first measured chymotrypsin-like activity of the proteasome over a wide range of Doxo concentrations in ARVM after 48 h incubation. The results showed no change at lower concentrations and a downregulation in the higher range when the majority of cells were TUNEL-positive (Figs. 2, 4). These initial results seemed to be at odds with publications by the group of Wang (Kumarapeli et al. 2005) who propose an activation of proteasome activity in the heart by anthracyclines. However, a time-course experiment with either a smaller concentration of 1 μM (considered clinically relevant by all investigators) or an extremely high dose has revealed that proteasome activity increases only initially and then decreases and that an extremely high Doxo concentration leads only to the inhibition of the activity or to the degradation of the proteasome itself, as indicated by the Western blotting experiment for 20S proteasome proteins. Inadequate proteolytic function of the ubiquitin-proteasome system might then lead to the activation of autophagy. Polyubiquitinated proteins were increased by Doxo treatment in our experiments and were clearly recognized as aggregates in cardiomyocytes showing concomitant myofibrillar changes. The mRNA of the sarcomere-associated ubiquitin ligase MURF-1 was found to be decreased at all concentrations of Doxo in ARVM. Interestingly, muscle actin is polyubiquitinated in vitro and in vivo and is targeted for breakdown by MURF-1 (Polge et al. 2011). Another E3 ubiquitin ligase important in muscle atrophy, atrogin-1, has been found to be increased by Doxo in neonatal rat cardiomyocytes and in mice but not MURF-1 (Yamamoto et al. 2008). Considering the previously observed myofibrillar degradation by the activation of calpain-1 and the presence of damaged mitochondria even at lower concentrations of Doxo in ARVM, the need for the removal of protein "waste" after anthracycline exposure is evident. Autophagy is able to remove protein aggregates to some extent, as has been reported in a study of glucose deprivation of cultured neonatal cardiomyocytes and autophagy inhibitors such as 3-methyladenine worsen the state of the cells (Marambio et al. 2010). However, this pro-survival system might become excessively active and lead to apoptosis as a consequence of maladaptive autophagy.

Our study has confirmed the need for an efficient and intact system of protein "waste" removal in adult mammalian cardiomyocytes under cytotoxic stress conditions such as anthracycline cancer therapy. Both the ubiquitin-proteasome system and autophagy are challenged in this situation and even if the amount of drugs might not reach the same higher concentration in the hearts of patients as under some of our experimental conditions, a repeated exposure carries the risk of cellular injury and cell death. However, encouragingly, new tools and therapies are currently in development for assessing autophagic activity in order either to limit excessive activation or to use the activation of this cellular pathway as a potential cardioprotective strategy in patients.

Acknowledgements We thank Franziska Seifriz for excellent technical assistance and Daniel Ott for contributions to Fig. 4.

References

Aapro M, Bernard-Marty C, Brain EG, Batist G, Erdkamp F, Krzemieniecki K, Leonard R, Lluch A, Monfardini S, Ryberg M, Soubeyran P, Wedding U (2011) Anthracycline cardiotoxicity in the elderly cancer patient: a SIOG expert position paper. Ann Oncol 22:257–267

Adams V, Linke A, Wisloff U, Doring C, Erbs S, Krankel N, Witt CC, Labeit S, Muller-Werdan U, Schuler G, Hambrecht R (2007) Myocardial expression of Murf-1 and MAFbx after induction of chronic heart failure: effect on myocardial contractility. Cardiovasc Res 73:120–129

Barth S, Glick D, Macleod KF (2010) Autophagy: assays and artifacts. J Pathol 221:117–124

Bristow MR, Billingham ME, Mason JW (1984) Adriamycin cardiotoxicity. Am J Cardiol 53:263–264

Bulteau AL, Szweda LI, Friguet B (2002) Age-dependent declines in proteasome activity in the heart. Arch Biochem Biophys 397:298–304

De Meyer GR, De Keulenaer GW, Martinet W (2010) Role of autophagy in heart failure associated with aging. Heart Fail Rev 15:423–430

Doroshow JH, Davies KJ (1986) Redox cycling of anthracyclines by cardiac mitochondria. II. Formation of superoxide anion, hydrogen peroxide, and hydroxyl radical. J Biol Chem 261:3068–3074

Eppenberger HM, Zuppinger C (1999) In vitro reestablishment of cell-cell contacts in adult rat cardiomyocytes. Functional role of transmembrane components in the formation of new intercalated disk-like cell contacts. FASEB J 13(Suppl):S83–S89

Fujimuro M, Yokosawa H (2005) Production of antipolyubiquitin monoclonal antibodies and their use for characterization and isolation of polyubiquitinated proteins. Methods Enzymol 399:75–86

Gevers W (1984) Protein metabolism of the heart. J Mol Cell Cardiol 16:3–32

Gewirtz DA (1999) A critical evaluation of the mechanisms of action proposed for the antitumor effects of the anthracycline antibiotics adriamycin and daunorubicin. Biochem Pharmacol 57:727–741

Glick D, Barth S, Macleod KF (2010) Autophagy: cellular and molecular mechanisms. J Pathol 221:3–12

Goorin AM, Chauvenet AR, Perez-Atayde AR, Cruz J, McKone R, Lipshultz SE (1990) Initial congestive heart failure, six to ten years after doxorubicin chemotherapy for childhood cancer. J Pediatr 116:144–147

Gregorio CC, Perry CN, McElhinny AS (2005) Functional properties of the titin/connectin-associated proteins, the muscle-specific RING finger proteins (MURFs), in striated muscle. J Muscle Res Cell Motil 26:389–400

Grune T, Jung T, Merker K, Davies KJ (2004) Decreased proteolysis caused by protein aggregates, inclusion bodies, plaques, lipofuscin, ceroid, and "aggresomes" during oxidative stress, aging, and disease. Int J Biochem Cell Biol 36:2519–2530

Hein S, Arnon E, Kostin S, Schonburg M, Elsasser A, Polyakova V, Bauer EP, Klovekorn WP, Schaper J (2003) Progression from compensated hypertrophy to failure in the pressure-overloaded human heart: structural deterioration and compensatory mechanisms. Circulation 107:984–991

Hilenski LL, Terracio L, Haas AL, Borg TK (1992) Immunolocalization of ubiquitin conjugates at Z-bands and intercalated discs of rat cardiomyocytes in vitro and in vivo. J Histochem Cytochem 40:1037–1042

Huang C, Zhang X, Ramil JM, Rikka S, Kim L, Lee Y, Gude NA, Thistlethwaite PA, Sussman MA, Gottlieb RA, Gustafsson AB (2010) Juvenile exposure to anthracyclines impairs cardiac progenitor cell function and vascularization resulting in greater susceptibility to stress-induced myocardial injury in adult mice. Circulation 121:675–683

Kabeya Y, Mizushima N, Ueno T, Yamamoto A, Kirisako T, Noda T, Kominami E, Ohsumi Y, Yoshimori T (2000) LC3, a mammalian homologue of yeast Apg8p, is localized in autophagosome membranes after processing. EMBO J 19:5720–5728

Klionsky DJ, Abeliovich H, Agostinis P, Agrawal DK, Aliev G, Askew DS, Baba M, Baehrecke EH, Bahr BA, Ballabio A, Bamber BA, Bassham DC et al (2008) Guidelines for the use and interpretation of assays for monitoring autophagy in higher eukaryotes. Autophagy 4:151–175

Knaapen MW, Davies MJ, De Bie M, Haven AJ, Martinet W, Kockx MM (2001) Apoptotic versus autophagic cell death in heart failure. Cardiovasc Res 51:304–312

Kondo RP, Apstein CS, Eberli FR, Tillotson DL, Suter TM (1998) Increased calcium loading and inotropy without greater cell death in hypoxic rat cardiomyocytes. Am J Physiol 275:H2272–H2282

Konorev EA, Vanamala S, Kalyanaraman B (2008) Differences in doxorubicin-induced apoptotic signaling in adult and immature cardiomyocytes. Free Radic Biol Med 45:1723–1728

Kostin S, Pool L, Elsasser A, Hein S, Drexler HC, Arnon E, Hayakawa Y, Zimmermann R, Bauer E, Klovekorn WP, Schaper J (2003) Myocytes die by multiple mechanisms in failing human hearts. Circ Res 92:715–724

Kobayashi S, Volden P, Timm D, Mao K, Xu X, Liang Q (2010)Transcription factor GATA4 inhibits doxorubicin-induced autophagy and cardiomyocyte death. J Biol Chem 285:793–804

Kumarapeli AR, Horak KM, Glasford JW, Li J, Chen Q, Liu J, Zheng H, Wang X (2005) A novel transgenic mouse model reveals deregulation of the ubiquitin-proteasome system in the heart by doxorubicin. FASEB J 19:2051–2053

Lebrecht D, Walker UA (2007) Role of mtDNA lesions in anthracycline cardiotoxicity. Cardiovasc Toxicol 7:108–113

Lim CC, Zuppinger C, Guo X, Kuster GM, Helmes M, Eppenberger HM, Suter TM, Liao R, Sawyer DB (2004) Anthracyclines induce calpain-dependent titin proteolysis and necrosis in cardiomyocytes. J Biol Chem 279:8290–8299

Marambio P, Toro B, Sanhueza C, Troncoso R, Parra V, Verdejo H, Garcia L, Quiroga C, Munafo D, Diaz-Elizondo J, Bravo R, Gonzalez MJ et al (2010) Glucose deprivation causes oxidative stress and stimulates aggresome formation and autophagy in cultured cardiac myocytes. Biochim Biophys Acta 1802:509–518

Mizushima N, Yamamoto A, Hatano M, Kobayashi Y, Kabeya Y, Suzuki K, Tokuhisa T, Ohsumi Y, Yoshimori T (2001) Dissection of autophagosome formation using Apg5-deficient mouse embryonic stem cells. J Cell Biol 152:657–668

Mrosek M, Labeit D, Witt S, Heerklotz H, Castelmur E von, Labeit S, Mayans O (2007) Molecular determinants for the recruitment of the ubiquitin-ligase MuRF-1 onto M-line titin. FASEB J 21:1383–1392

Nemchenko A, Chiong M, Turer A, Lavandero S, Hill JA (2011) Autophagy as a therapeutic target in cardiovascular disease. J Mol Cell Cardiol 51:584–593

Nishida K, Kyoi S, Yamaguchi O, Sadoshima J, Otsu K (2009) The role of autophagy in the heart. Cell Death Differ 16:31–38

Poindexter BJ, Smith JR, Buja LM, Bick RJ (2001) Calcium signaling mechanisms in dedifferentiated cardiac myocytes: comparison with neonatal and adult cardiomyocytes. Cell Calcium 30:373–382

Polge C, Heng AE, Jarzaguet M, Ventadour S, Claustre A, Combaret L, Bechet D, Matondo M, Uttenweiler-Joseph S, Monsarrat B, Attaix D, Taillandier D (2011) Muscle actin is polyubiquitinylated in vitro and in vivo and targeted for breakdown by the E3 ligase MuRF1. FASEB J 25:3790–3802

Powell SR (2006) The ubiquitin-proteasome system in cardiac physiology and pathology. Am J Physiol Heart Circ Physiol 291:H1–H19

Powell SR, Wang P, Divald A, Teichberg S, Haridas V, McCloskey TW, Davies KJ, Katzeff H (2005) Aggregates of oxidized proteins (lipofuscin) induce apoptosis through proteasome inhibition and dysregulation of proapoptotic proteins. Free Radic Biol Med 38:1093–1101

Ranek MJ, Wang X (2009) Activation of the ubiquitin-proteasome system in doxorubicin cardiomyopathy. Curr Hypertens Rep 11:389–395

Sawyer DB, Peng X, Chen B, Pentassuglia L, Lim CC (2010) Mechanisms of anthracycline cardiac injury: can we identify strategies for cardioprotection? Prog Cardiovasc Dis 53:105–113

Singal P, Iliskovic N (1998) Doxorubicin-induced cardiomyopathy. N Engl J Med 339:900–905

Steinherz LJ, Steinherz PG, Tan CT, Heller G, Murphy ML (1991) Cardiac toxicity 4 to 20 years after completing anthracycline therapy. JAMA 266:1672–1677

Tannous P, Zhu H, Nemchenko A, Berry JM, Johnstone JL, Shelton JM, Miller FJ Jr, Rothermel BA, Hill JA (2008) Intracellular protein aggregation is a proximal trigger of cardiomyocyte autophagy. Circulation 117:3070–3078

Timolati F, Anliker T, Groppalli V, Perriard JC, Eppenberger HM, Suter TM, Zuppinger C (2009) The role of cell death and myofibrillar damage in contractile dysfunction of long-term cultured adult cardiomyocytes exposed to doxorubicin. Cytotechnology 61:25–36

Tokarska-Schlattner M, Zaugg M, Zuppinger C, Wallimann T, Schlattner U (2006) New insights into doxorubicin-induced cardiotoxicity: the critical role of cellular energetics. J Mol Cell Cardiol 41:389–405

Wang X, Su H, Ranek MJ (2008) Protein quality control and degradation in cardiomyocytes. J Mol Cell Cardiol 45:11–27

Weinberg LE, Singal PK (1987) Refractory heart failure and age-related differences in adriamycin-induced myocardial changes in rats. Can J Physiol Pharmacol 65:1957–1965

Xie M, Morales CR, Lavandero S, Hill JA (2011) Tuning flux: autophagy as a target of heart disease therapy. Curr Opin Cardiol 26:216–222

Yamamoto Y, Hoshino Y, Ito T, Nariai T, Mohri T, Obana M, Hayata N, Uozumi Y, Maeda M, Fujio Y, Azuma J (2008) Atrogin-1 ubiquitin ligase is upregulated by doxorubicin via p38-MAP kinase in cardiac myocytes. Cardiovasc Res 79:89–96

Zhang J, Clark JR Jr, Herman EH, Ferrans VJ (1996) Doxorubicin-induced apoptosis in spontaneously hypertensive rats: differential effects in heart, kidney and intestine, and inhibition by ICRF-187. J Mol Cell Cardiol 28:1931–1943

Zhu H, Tannous P, Johnstone JL, Kong Y, Shelton JM, Richardson JA, Le V, Levine B, Rothermel BA, Hill JA (2007) Cardiac autophagy is a maladaptive response to hemodynamic stress. J Clin Invest 117:1782–1793